Cellular and Molecular Biology
E-ISSN : 1165-158X / P-ISSN : 0145-5680
www.cellmolbiol.org

Evaluation of vincamine against acetylcholinesterase enzyme

Syed Sayeed Ahmad[1], Aisha Khatoon[2], Mohd. Sajid Khan[2], Mohammad Khalid[3], Ahmed M. Alharbi[4], Mohd. Haris Siddiqui[1*]

[1] Department of Bioengineering, Integral University, Lucknow 226026, India
[2] Department of Biosciences, Faculty of Science, Integral University, Lucknow 226026, India
[3] College of Pharmacy, Department of Pharmacognosy, Prince Sattam Bin Abdul Aziz university, Alkharj 16278, Riyadh, Saudi Arabia
[4] Department of Clinical Laboratory Sciences, College of Applied Medical Sciences, University of Hail, Hail, Saudi Arabia

ARTICLE INFO

Original paper

Article history:
Received: April 07, 2022
Accepted: July 04, 2022
Published: July 31, 2022

Keywords:

Natural compound, AChE, Alzheimer's disease, Vincamine, IC_{50} value; inhibition kinetic

ABSTRACT

The current article deals with the *in-silico* along with enzyme kinetics approach to search for a prominent AChE enzyme inhibitor among the known natural compounds. The computational tools were involved for this purpose and eventual vincamine, a monoterpenoid indole alkaloid, was selected based on several parameters, including free energy of binding (-10.77 kcal/mol) and ADME parameter. Computationally, it confirmed the interaction between vincamine and AChE at an indistinguishable locus from that of substrate AChI (-3.94 kcal/mol) but with much higher binding energy. Interestingly, amino acid residues Gly120, Gly121, Gly122, Glu202, Trp86, Tyr133, Ser203, Phe297, and His447 of AChE were found to be common in these interactions. Further, these findings were approved with wet lab tests where detailed kinetics was studied. It was found that vincamine inhibited AChE with the inhibition constant K_i (239 µM). The value of IC_{50} (239 µM) and K_M (0.598 mM) was determined and further confirmed by Dixon, Lineweaver- Burk reciprocal, Hanes, and Eadie-Hofstee plots, respectively. The mode of interaction of the compound was found to be competitive for AChE. Thus, the present computational and enzyme kinetics studies conclude that vincamine can be a promising inhibitor of AChE for the effective management of AD.

Doi: http://dx.doi.org/10.14715/cmb/2022.68.7.3

Introduction

Alzheimer's disease (AD) is a progressive, irreversible neurodegenerative disorder that causes the death of brain cells and is recognized as a reason for dementia in elderly people (1). In the future, of around 8-10 years, AD is getting to be a standout amongst the most expensive maladies for society (2). AD is an intricate disorder where distinctive variables like β-amyloid conglomeration, deficiency of acetylcholine (ACh), and accumulation of tau proteins are considered as in charge of its etiology (3, 4). AD is characterized by severe loss of cholinergic neurons located in the basal forebrain and reduced ACh uptake in the cortical and hippocampus region of the brain. The cholinergic breakdown and its serious impact on AD gives a method of reasoning to the helpful utilization of acetylcholinesterase (AChE) inhibitors (5). AD can be treated by the employment of specific AChE inhibitors (6). The principle ability of AChE is to stop the working of ACh and ends the signaling at cholinergic neural connections. Besides, AChE increases the accumulation of β amyloid protein in the cerebrum, which is responsible for the development of AD (7). In various studies, it has already been proved that AChE inhibitors played a vital role in the treatment of AD by preventing the degradation of ACh (8, 9). Cholinesterase inhibitors are not regularly utilized as a part of allopathic medicine and current medications don't prompt adequate generation of ACh in the treatment of AD. The phytochemicals and natural compounds, due to their antioxidant and anti-aging properties, are widely explored in the treatment of neurodegenerative disorders (10). Vincamine is a monoterpenoid indole alkaloid obtained from *Vinca minor* leaves having potent vasodilator action which increases the blood circulation to the cerebrum. It is also used for neuroprotective qualities, improvement, and antitumor impact of its subsidiaries. Vincamine is generally utilized as a part of human pharmaceuticals to increase the bloodstream in patients with acute or subchronic cerebral ischemia (11). Vincamine has already been studied as a potent AChE inhibitor by various groups of researchers. Ilkay Orhan et al; studied in vitro anticholinesterase activity of various plant alkaloids and concluded vincamine as a potent candidate to inhibit cholinesterase enzyme (12). Similarly, Omar M. E. Abdel-Salam et al; confirmed the effect of vincamine in the treatment of neurodegenerative disorder due to cholinesterase inhibitory action (13). All these reported studies were mainly focused on the evaluation of vincamine as an AChE inhibitor. Through an extensive literature search, it has also been observed that very little or no work has been done on computational studies, including molecular docking, molecular properties, drug-likeness, type of enzyme inhibition, and kinetic assay study of vincamine. A detailed and extensive in vitro study coupled with a computational study could be a

* Corresponding author. Email: mohdharis.siddiqui@gmail.com

great advancement towards the improvement of increasing powerful AChE inhibitors for the treatment of AD. Thus, in this research work, we have evaluated the anti-Alzheimer potential of natural compound vincamine using an *in-silico* approach along with enzyme kinetics study.

Materials and Methods

Computational study

Target preparation for molecular interaction analysis

The human AChE (PDB ID: 3LII) enzyme (Figure 1.a) information was collected from the Protein Data bank (PDB) by a resolution of 3.2Å (http://www.rcsb.org/pdb/home/home.do). Ligands, water, and other heteroatoms were expelled from the protein atom alongside the other chain.

Ligand preparation for molecular docking study

Vincamine was used as the ligand in this study and its chemical structure (PubChem CID:15376) (Figure 1.b) was collected from the PubChem database (http://pubchem.ncbi.nlm.nih.gov) and further, it was saved in PDB format.

Molecular properties and drug-likeness

Drug-likeness is a key consideration when choosing compounds for the beginning periods of medication disclosure (14). The compounds with 5 and 0 hydrogen bond donors and acceptors, respectively, 500-dalton molecular mass and 5 log P value are considered as drug-likeness as per Lipinski's rule of five, which is also known as the rule of five (ROF). SwissADME (http://www.swissadme.ch/index.php) was used to calculate the molecular properties of the compound.

Molecular docking and visualization

The docking process with an inhibitory compound (Vincamine) against AChE was done via AutoDock4.2. Protein and ligands were analyzed and adjusted for docking by utilizing AutoDock Tools which is incorporated in the MGL devices (http://mgltools.scripps.edu). The examination of the binding adaptation of ligand-protein complexes was performed utilizing a scoring capacity and free binding energy (15). The docking was performed on protein molecules with the incorporation of polar hydrogen atoms and characterization of rotatable bonds was performed. Further, the Auto Dock tool was used to incorporate hydrogen atoms, Kollman joined particles compose charges and salvation constraint. Auto grid program was used to create affinity grid maps of the dimensions of 40 x 40 x 40 Å matrix to target lattice co-ordinates through AChE active sites. For AChE, the x, y, and z co-ordinates on the catalytic site were 90.81, 83.98, and -8.04, respectively (16). Van der Waals and electrostatic terms were counted independently using separation subordinate dielectric capacities at automated dock mode using 'Lamarckian genetic algorithm with 10 unique runs and ended after 2,500,000 energy assessments. After AutoDock execution, the ligand-receptor complex was confirmed 10 times and the complex was visualized using the discovery studio visualizer and finally, binding energy was determined.

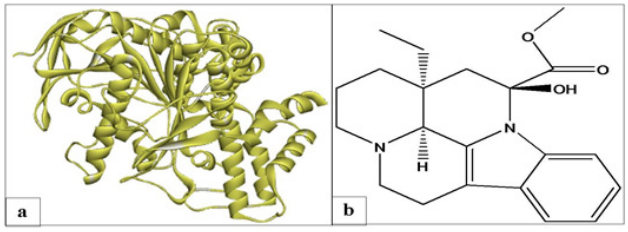

Figure 1. Structure of the selected molecule (a) target enzyme (b) ligand Vincamine.

Wet lab study

Materials

Dimethyl sulfoxide (DMSO), 5,5-dithio-bis-(2-nitrobenzoic acid) (DTNB), Tris buffer, Acetylcholine iodide (AChI), and Acetylcholinesterase enzyme (AChE) were obtained from Sigma–Aldrich Co., Magnesium Chloride ($MgCl_2$) Sodium Chloride (NaCl), vincamine used as per obtained.

In vitro inhibition studies on AChE

The Ingkaninan method was employed to calculate the enzymatic activity (17). In this method, 3 ml reaction mixture was prepared by mixing DTNB (3 mM, 1000µl), AChI (15 mM, 200 µl), Tris-HCl buffer (50 mM/pH 8, 700 µl), and 1 AChE (0.25 Uml^{-1}, 50 µl) in a test tube and different concentration of vincamine were used. The reaction mixture was placed in a cuvette and different concentrations of vincamine were added. The response was observed spectrometrically for 10 min at 405 nm. The reaction mixture (3ml) without vincamine was worked as blank. The % inhibition of AChE activity was determined with the help of the subsequent mentioned procedure:

$$\text{Percentage inhibition} = \frac{(\Delta \text{ OD of Control} - \Delta \text{ OD of Drug})}{\Delta \text{ OD of Control}} \times 100$$

Kinetic Assay

The kinetic assay study of vincamine was carried out at five different concentrations (5, 5.5, 7.5, 8.5, and 10mM) of acetylcholine iodide (AChI) in the presence and absence of vincamine at three concentrations (150, 200, and 250 µM) in three different reactions. The samples were analyzed spectrometrically at 405 nm for 10 min and OD at each minute was recorded and a Lineweaver-Burk graph was plotted to draw the line of inhibition. The equation is presented below:

$$\frac{1}{V} = \frac{K_m}{V_{max}} \cdot \frac{1}{[S]} + \frac{1}{V_{max}} \quad (1)$$

The secondary plots were plotted using the following formula.

$$K'_m = \frac{K_m}{K_i}[I] + K_m \quad (2)$$

Again, the Hanes plot was plotted using the following formula.

$$\frac{[S]}{V} = \frac{[S]}{V_{max}} + \frac{K_m}{V_{max}} \quad (3)$$

Estimation of Ki using Dixon plots

The Dixon plot was used to determine the type of enzyme inhibitions and dissociation constant Ki. Graphs were plotted between 1/V versus [I] at every [S]. The condition utilized for this association is specified below

$$\frac{1}{v} = \frac{K_m}{V_{max}[S]} \cdot \frac{I}{K_i} + \frac{K_m}{V_{max}[S]} + \frac{1}{V_{max}} \quad (4)$$

The value of K_i was acquired by simultaneously solving two sets of equations successively. The purpose of the crossing point of these sets of lines expresses in the estimation of Ki (Fig. 7).

Results and Discussion

In this work, *in vitro* enzyme inhibition and enzyme kinetic study have been assumed as an endeavor to examine the capacity of vincamine to go about as a strong AChE inhibitor and to illuminate the potential mechanism of accomplishment. In the meantime, the inhibitory actions of vincamine against AChE are still unknown. Thus, the binding mechanism of vincamine inhibitor was studied by different methodologies comprising of molecular docking approach, enzyme inhibition analysis, and enzyme kinetic studies. We strongly believe that this exploration would be helpful for analysts associated with medication planning in their continuous look for strong and adaptable AChE inhibitors. Furthermore, the ramifications of conceivable restraint by a compound might assist in the improvement of novel medications that show the anti-Alzheimer's activity.

Molecular Interaction Study

This work depicts the molecular connections along with human AChE and vincamine, which were screened from 300 natural compounds based on binding efficiency with the selected target. Docking has turned out to be one of the essential strategies for lead compound improvement. Molecular docking is one of the best methods to determine the binding mechanism and affinity of the ligand with the protein molecule (18). The active compounds that do not fit properly in the binding site can also be recognized in molecular docking (19, 20). It is merit specifying that the "ligand" and "protein" were held adaptable by the docking programming throughout the study. AChE, with its catalytic anionic locations (ACS) interacted with vincamine through 18 amino acids, specifically Asp74, Asn87, Gln71, Gly120, Gly121, Gly122, Gly126, Glu202, Tyr72, Trp86, Tyr124, Tyr133, Tyr337, Ser125, Ser203, Phe297, Phe338 and His447 (Figure 2). In our study, the free binding energy of -10.77 kcal/mol for vincamine-AChE CAS interaction was observed. Vincamine was seen to be engaged with four hydrogen bonding as UNK0:H45 - TYR124:OH, TYR124:OH - UNK0:O1, TYR124:OH - UNK0:O2, and TYR337:OH - UNK0:O1 at the active site of AChE. In a current report, the –OH of Tyr124 likewise demonstrated a hydrogen bond. The CAS containing the Ser-His-Glu set of the catalytic chord has a distinctive direction beside the dynamic site gorge, stretching out from the CAS, on the base close to Trp86 (21).

C11 and C12 carbon atoms of vincamine were involved in hydrophobic interactions through CE2 and CZ of residues Tyr124 and Tyr72 of the enzyme, respectively. C18 of vincamine was observed in pi-pi interactions with CE2 and CZ of the Tyr72 amino acid residue. Van der Waals, hydrogen bond and desolvation energy components of vincamine interface with AChE were found to be -11.22 kcal/mol, and electrostatic energy of -0.74 Kcal/mol was observed, while vincamine –AchE complex interface surface area of 890.952 Å^2 was observed. It is seen that a perfect AChE inhibitor should attach to the reactant destinations, which possibly will disturb the communications among the protein and peptide (Aβ) and slow down the malady movement (22). Hydrogen bonds, hydrophobic bonds, and pi-pi interactions assumed an imperative part of the vincamine-AChE interaction.

Substrate AChI was docked into a similar location to AChE. In this study, amino acid residues, Trp86, Gly120, Gly121, Gly122, Tyr133, Glu202, Ser203, Phe295, Phe297, His447, Gly448, and Ile451 assumed a noteworthy function in the binding of AChI. Interestingly, amino acid residues, Trp86, Gly120, Gly121, Gly122, Tyr133, Glu202, Ser203, Phe297, and His447 of AChE were also observed to be associated with the interface with vincamine. The free binding energy of -3.94kcal/mol for 'AChI -AChE CAS-interaction' was observed. Van der Waals, hydrogen bond and desolvation energy components of AChI interaction with AChE were found to be -4.23 kcal/mol and electrostatic energy segment of -0.03kcal/mol was observed, while AChI-AChE complex total involved surface area of 652.511 Å^2 was found. The estimated free binding energy (ΔG) for substrate-AChE and vincamine-AChE interaction were -3.94kcal/mol and -10.77 kcal/mol, respectively and can propose the proficiency of the complex (23).

This special action of vincamine showed competitive binding nature towards the catalytic sites of AChE. The selected natural compound vincamine has the highest drug-likeness score of 1.18. FDA-approved drug tacrine has a value of 0.97. The general medication likeliness score for drug constitute is right-skewed and tops in the scope of 0.8 to 1.2 (24) represented by Figure3.

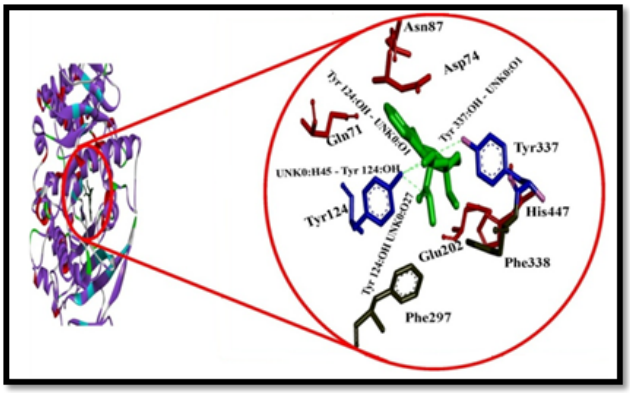

Figure 2. Interaction of vincamine docked to AChE. The ligand vincamine has been shown in the 'green color stick' representation.

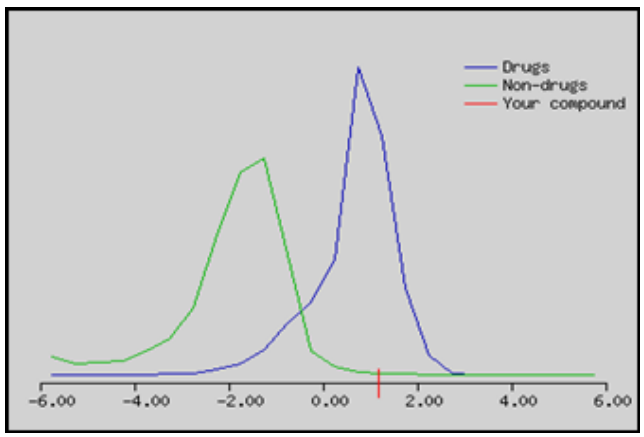

Figure 3. Graph representing the Drug-likeness model score.

It was accounted that the hydrogen bonding formed between compound and protein most of the time gives constancy to the ligand-protein complex and these formed hydrogen bonds are responsible for the stability of the complex (25, 26).

Enzyme kinetics study

The inhibition kinetics studies were endeavored to clarify how an inhibitor follows up on the catalyst and predicts its adequacy. The kinetic constants Km and Ki are basic to understanding enzymatic activity in controlling the metabolism of an organism. We considered enzyme inhibition kinetics of vincamine on AChE along with the computational study.

The selected inhibitor showed noteworthy concentration-dependent restraint of AChE utilizing AChI as a substrate. The Michaelis-Menten constant Km was dictated by the Lineweaver-Burk plan (27), in which substrate hydrolysis inverse (1/V) of inhibitor concentration was designed against substrate concentrations inverse by appropriating data in ORIGIN 6.1 (Figure 4). Further, the Ki of the interaction was determined by Lineweaver and Burk's plot using the equation to confirm with Dixon plot.

$$\frac{V}{[S]} = \frac{V_{max} - V}{K_m} \quad (5)$$

Lineweaver Burk plot has been used for the acknowledgment of competitive, non-competitive, and uncompetitive inhibitors. In experimental observations, the compound showed competitive inhibition that has a comparable y-intercept as uninhibited there are diverse slopes and x-intercepts between the distinctive informational data.

The AChE activity was estimated at various concentrations of substrate AChI (5, 5.5, 7.5, 8.5, and 10 mM). The concentration-dependent competitive inhibition of AChE was observed for vincamine through Line Weaver-Burk reciprocal plot without affecting Vmax. The K_m value for the AChE with AChI was found to be 0.598mM and the same was further confirmed by the secondary graph (Figure 8b), Eadie- Hofstee (28), and Hanes plots (29). Eadie-Hofstee plot was utilized truly for fast distinguishing proof of critical kinetic terms like K_M and V_{max}. Eadie-Hofstee's design is a graphical portrayal of kinetics which is plotted in between V against V/[S] for the K_m value as a negative slope which was found to be 0.598mM (Figure 5).

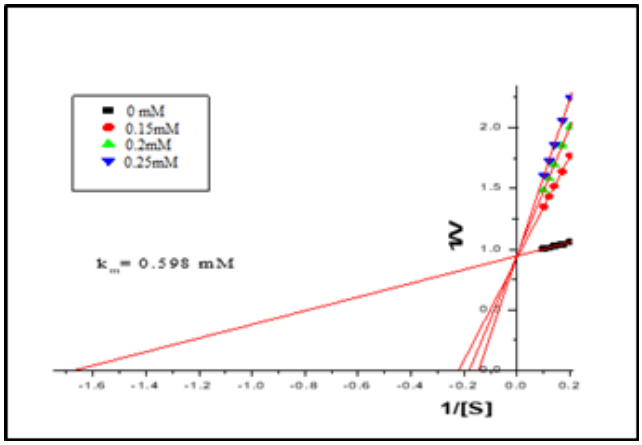

Figure 4. Concentration-dependent AChE inhibition by vincamine using Lineweaver-Burk plot.

$$\frac{1}{Km'} = \frac{1}{Km\left(1+\frac{I}{Ki}\right)} \quad (6)$$

Hanes Plot depends on the reworking of the Michaelis–Menten representation. It is the proportion of the underlying [S] to response velocity, V, which was plotted against [S] for the determination of the K_m value (Figure 6).

The estimation of Ki was dictated by the Dixon (30) plot between the inverse of substrate hydrolysis (1/v) and [I] and appropriates the data in software (Figure 7). The value for Ki was acquired from the convergence of the line depicted by that substrate concentration and the line having the slightest slope that is the greatest substrate concentration.

The obtained value of K_i from the Dixon plot was found to be 239µM and it was also confirmed by secondary plots (Figure 8.a,b).

The half-maximal inhibitory concentration (50% inhibitory concentration) has been utilized to study the restraint energy of an enzymatic response and to characterize the adequacy of an inhibitor (31). The AChE action was estimated at various concentrations of vincamine (150, 200, and 250 µM). The vincamine inhibited AChE with an IC_{50} value of 239µM by appropriate information with ORIGIN 6.1 in Figure 9.

Similarly, an alkaloid isolated from Nigerian Crinum

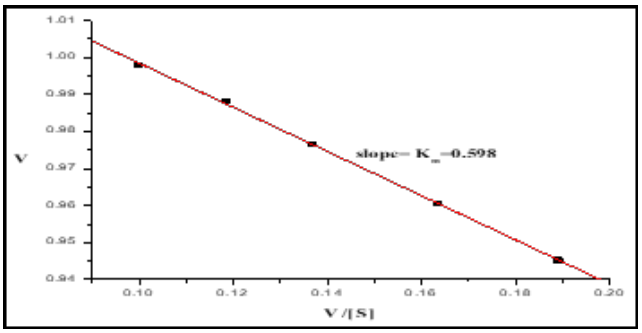

Figure 5. Eadie- Hofstee plot.

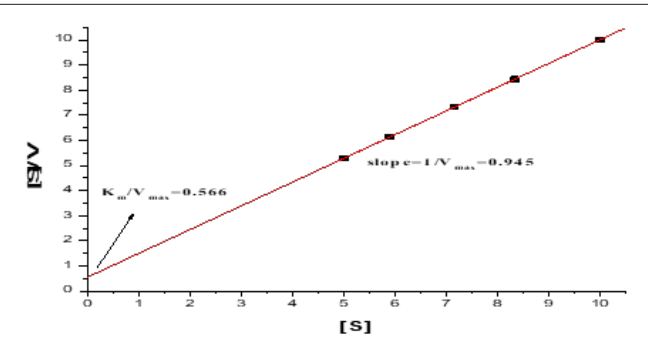

Figure 6. Hanes plots.

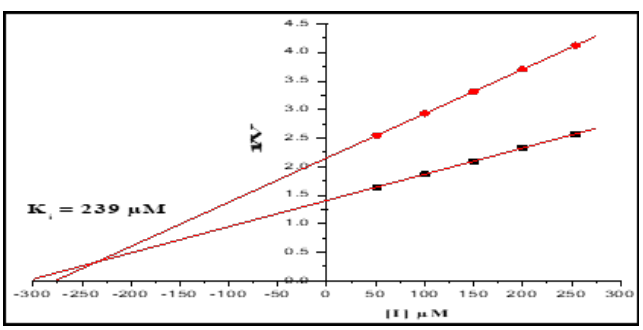

Figure 7. Dixon's Plot of inhibition of AChE by vincamine.

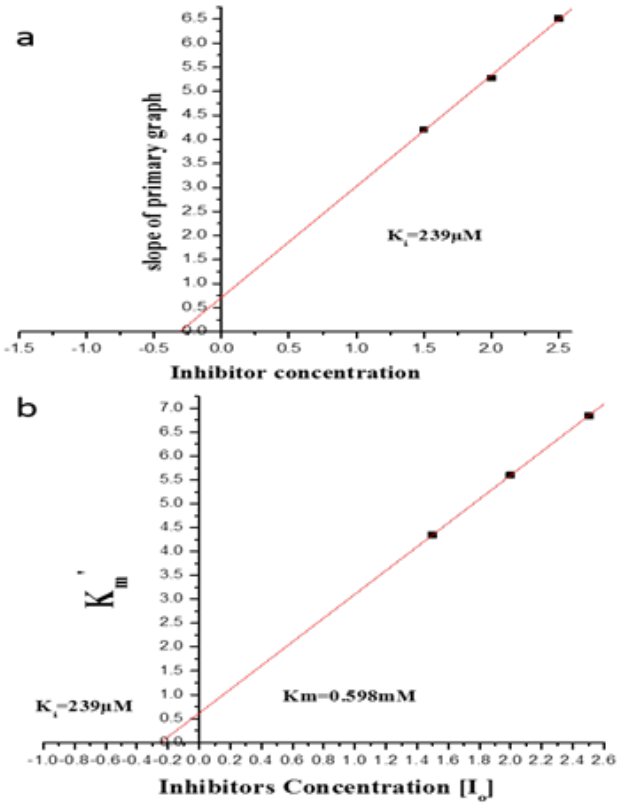

Figure 8. Secondary plot showed **(a)** inhibition constant and **(b)** inhibition constant Ki & Km.

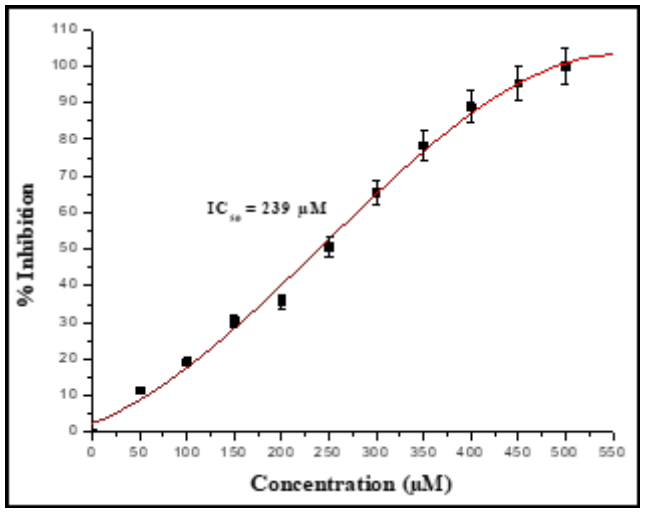

Figure 9. AChE inhibition curves for vincamine.

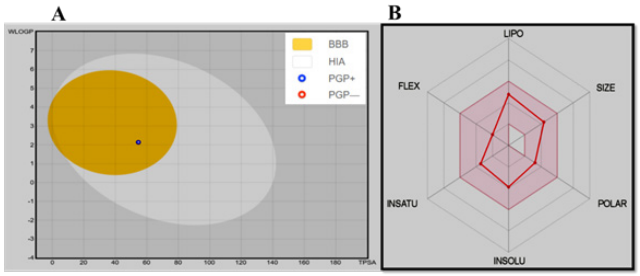

Figure 10. Molecular properties of vincamine**. A).** representing the status of BBB and HIA, **B).** vincamine following Bioavailability Radar.

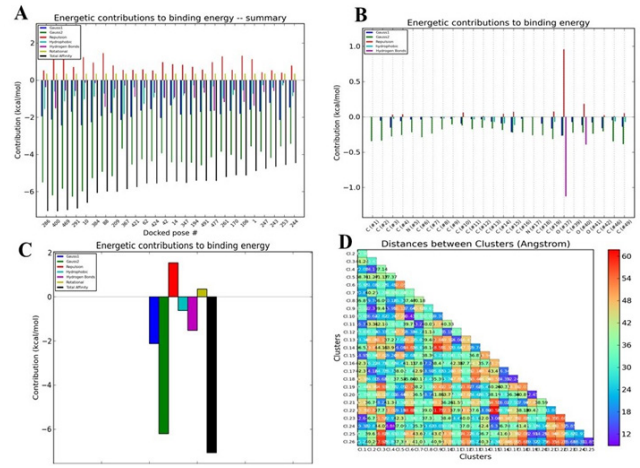

Figure 11. Binding energy contribution. **A).** energetic contribution to all the possible poses in the complex**, B).** energetic contribution to each atom of compound **C).** energetic contribution of best selected pose with maximum binding energy**, D).** distances between possible clusters in the selected complex.

species, hamayne exhibited an IC_{50} value of 250 µM, three derivatives of tetrahydroquinolines also showed IC_{50} values of 215 µM, 805 µM, and 618 µM against AChE, and lycorine show 450 µM as IC_{50} value (32, 33). Since the value of K_m increases with an increase in competitive inhibition. Similarly, one of the acetonitrile compounds was also found to increase Km value (0.699 mM) for the same substrate (34), which is comparable to the Km value of vincamine against AChE. Herbal prescriptions have been a noteworthy source of novel compounds with different pharmaceutical exercises since the beginning (35, 36). Almost all the drugs have been derived, modified, or isolated from natural sources against several diseases, including AD. Vincamine, nowadays a leading drug, is utilized for cerebral metabolic and circulatory scatter disorders as it links hemodynamic and cerebrometabolic assets. Vincamine derivatives efficiently protect cells from the attack of reactive oxygen species (37-40). All the predicted values from different plots were summarized in Table 1.

Along with this study, several properties like absorption, distribution, metabolism, and excretion (ADME) were anticipated by SwissADME (41). Due to the unfavorable ADME parameter, several therapeutic compounds fail to reach clinical trials. Lipinski's rule (42), Veber's rule (43), Egan's rule (44), Polar surface area (TPSA), and rotatable bonds were predicted and are elucidated in Table 2. The HIA and BBB level of vincamine was shown in Figure 10 collectively. The selected compound followed all the properties as mentioned in Table 2.

Further, the Achilles Blind Docking server (45) (http://bio-hpc.eu/software/blind-docking-server/) was employed to confirm the interactions between AChE and vincamine, which were found to interact with each other with a binding score of -7.10 kcal/mol. Here energetic contribution to the binding energy for the selected complex with different formed docked pose numbers as shown in Figure 11 A, while Figure 11B represents the selected pose number with the highest binding energy with each atom of vincamine. Figure 11 C represents the highest binding energy pose, while Figure 11D represents the distances between each cluster.

Conclusions

In the present study, the free binding energy for vincamine and substrate was found to be -10.77kcal/mol and -3.94kcal/mol, correspondingly. Vincamine and substrate

Table 1. The obtained value of K_m, K_i, and IC_{50} from different plots.

Plots Name	Plots in between	K_m Value	K_i Value	IC_{50} Value
Lineweaver-Burk Plot	1/V Vs 1/[S]	0.598 mM	_____	_____
Dixon Plot	1/V Vs [I]	_____	239 µM	_____
Eadie-Hofstee Plot	V Vs V/[S]	0.598 mM	_____	_____
Hanes Plot	[S]/V Vs [S]	0.598 mM	_____	_____
secondary plot	K'_m Vs [I]	0.598 mM	239 µM	_____
secondary plot	The slope of primary graph Vs [I]	_____	239 µM	_____
Inhibition assay	% inhibition Vs [I]	_____	_____	239 µM

Table 2. Pharmacokinetic properties of Vincamine.

Properties		Vincamine
Physicochemical	Formula	C21H26N2O3
	Molecular weight	354.44 g/mol
	Number of heavy atoms	26
	Number of aromatic heavy atoms	9
	Number of rotatable bonds	3
	Number of H-bond acceptors	4
	Number of H-bond donors	1
	Molar Refractivity	103.74
	TPSA	54.70 Å²
Lipophilicity (Log Po/w)	iLOGP	2.81
	XLOGP3	2.86
	WLOGP	2.14
	MLOGP	2.62
	SILICOS-IT	2.60
	Consensus Log Po/w	2.61
Water Solubility	Log S (ESOL)	-3.90 (Soluble)
	Log S (Ali)	-3.67 (Soluble)
	Log S (SILICOS-IT)	-4.28 (Moderately soluble)
Pharmacokinetics	BBB permeant	Yes
	GI absorption	High
	Log Kp (skinpermeation)	-6.43 cm/s
Druglikeness	Lipinski	Yes
	Ghose	Yes
	Veber	Yes
	Egan	Yes
	Muegge	Yes
	Bioavailability Score	0.55

were complexed with the AChE at a similar locus. Interestingly, amino acid residues, Trp86, Gly120, Gly121, Gly122, Tyr133, Glu202, Ser203, Phe297, and His447 of AChE were exposed in common interaction with vincamine and AChI. In the enzyme inhibition assay, vincamine showed inhibition with an IC_{50} value of 250 µM. The Michaelis-Menten constant K_m was preliminarily resolute by the Lineweaver-Burk plot, which was found to be 0.598mM and the same was confirmed by Eadie- Hofstee and Hanes plots. The obtained value of K_i from the Dixon plot was found to be 239µM and, it was also confirmed by secondary plots. Line Weaver–Burk reciprocal plot demonstrated, that vincamine as a competitive inhibitor of AChE and K_m value was found to increase with concentration of inhibitor without affecting the V_{max}. Vincamine was found to satisfy drug-likeness properties in the in silico analysis. These findings clarify the valuable impacts of vincamine against AD and give a premise to the plan and improvement of the AChE inhibitor. A combination of *in-vitro* and computational study could be an imperative advance towards the improvement of increasingly powerful AChE inhibitors for the management of AD.

Acknowledgments
None

Conflict of interest
The authors confirm that this article content has no conflict of interest.

References

1. Ahmad SS, Akhtar S, Jamal QM, Rizvi SM, Kamal MA, Khan MK, Siddiqui MH. Multiple Targets for the Management

of Alzheimer's Disease. CNS Neurol Disord Drug Targets. 2016;15(10):1279-1289. doi: 10.2174/1871527315666161003165855

2. Alzheimer's Association. 2013 Alzheimer's disease facts and figures. Alzheimers Dement. 2013 Mar;9(2):208-45. doi: 10.1016/j.jalz.2013.02.003
3. Förstl H, Kurz A. Clinical features of Alzheimer's disease. Eur Arch Psychiatry Clin Neurosci. 1999;249(6):288-90. doi: 10.1007/s004060050101.
4. Melnikova I. Therapies for Alzheimer's disease. Nat Rev Drug Discov. 2007 May;6(5):341-2. doi: 10.1038/nrd2314.
5. Hitzeman N. Cholinesterase inhibitors for Alzheimer's disease. Am Fam Physician. 2006 Sep 1;74(5):747-9.
6. Chaves SKM, Afzal MI, Islam MT, Hameed A, Da Mata AMOF, Da Silva Araújo L, Ali SW, Rolim HML, De Medeiros MDGF, Costa EV, Salehi B, Martins N, Arif AM, Imran M, Sharifi-Rad J, Melo-Cavalcante AAC, Feitosa CM. Palmatine antioxidant and anti-acetylcholinesterase activities: A pre-clinical assessment. Cell Mol Biol (Noisy-le-grand). 2020 Jun 25;66(4):54-59. PMID: 32583771.
7. Citron M. Alzheimer's disease: strategies for disease modification. Nat Rev Drug Discov. 2010 May;9(5):387-98. doi: 10.1038/nrd2896.
8. Ahmad SS, Khan H, Khalid M, Almalki AS. Emetine and Indirubin- 3- monoxime interaction with human brain acetylcholinesterase: A computational and statistical analysis. Cell Mol Biol (Noisy-le-grand). 2022 Jan 2;67(4):106-114. doi: 10.14715/cmb/2021.67.4.12.
9. Adewusi EA, Moodley N, Steenkamp V. Antioxidant and acetylcholinesterase inhibitory activity of selected southern African medicinal plants. South African Journal of Botany. 2011 Aug 1;77(3):638-44. doi.org/10.1016/j.sajb.2010.12.009
10. Fusco D, Colloca G, Lo Monaco MR, Cesari M. Effects of antioxidant supplementation on the aging process. Clin Interv Aging. 2007;2(3):377-87.
11. Fandy TE, Abdallah I, Khayat M, Colby DA, Hassan HE. In vitro characterization of transport and metabolism of the alkaloids: vincamine, vinpocetine and eburnamonine. Cancer Chemother Pharmacol. 2016 Feb;77(2):259-67. doi: 10.1007/s00280-015-2924-3.
12. Orhan I, Naz Q, Kartal M, Tosun F, Sener B, Choudhary MI. In vitro anticholinesterase activity of various alkaloids. Z Naturforsch C J Biosci. 2007 Sep-Oct;62(9-10):684-8. doi: 10.1515/znc-2007-9-1010.
13. Abdel-Salam OM, Hamdy SM, Seadawy SA, Galal AF, Abouelfadl DM, Atrees SS. Effect of piracetam, vincamine, vinpocetine, and donepezil on oxidative stress and neurodegeneration induced by aluminum chloride in rats. Comparative Clinical Pathology. 2016 Mar;25(2):305-18.
14. Bickerton GR, Paolini GV, Besnard J, Muresan S, Hopkins AL. Quantifying the chemical beauty of drugs. Nat Chem. 2012 Jan 24;4(2):90-8. doi: 10.1038/nchem.1243.
15. Huey R, Morris GM, Olson AJ, Goodsell DS. A semiempirical free energy force field with charge-based desolvation. J Comput Chem. 2007 Apr 30;28(6):1145-52. doi: 10.1002/jcc.20634.
16. Shaikh S, Ahmad SS, Ansari MA, Shakil S, Rizvi SM, Shakil S, Tabrez S, Akhtar S, Kamal MA. Prediction of comparative inhibition efficiency for a novel natural ligand, galangin against human brain acetylcholinesterase, butyrylcholinesterase and 5-lipoxygenase: a neuroinformatics study. CNS Neurol Disord Drug Targets. 2014 Apr;13(3):452-9. doi: 10.2174/18715273113126660162.
17. Ingkaninan K, Temkitthawon P, Chuenchom K, Yuyaem T, Thongnoi W. Screening for acetylcholinesterase inhibitory activity in plants used in Thai traditional rejuvenating and neurotonic remedies. J Ethnopharmacol. 2003 Dec;89(2-3):261-4. doi: 10.1016/j.jep.2003.08.008.
18. Klebe G. Virtual ligand screening: strategies, perspectives and limitations. Drug Discov Today. 2006 Jul;11(13-14):580-94. doi: 10.1016/j.drudis.2006.05.012.
19. Oprea TI, Matter H. Integrating virtual screening in lead discovery. Curr Opin Chem Biol. 2004 Aug;8(4):349-58. doi: 10.1016/j.cbpa.2004.06.008.
20. Mizutani MY, Itai A. Efficient method for high-throughput virtual screening based on flexible docking: discovery of novel acetylcholinesterase inhibitors. J Med Chem. 2004 Sep 23;47(20):4818-28. doi: 10.1021/jm030605g.
21. Fang J, Wu P, Yang R, Gao L, Li C, Wang D, Wu S, Liu AL, Du GH. Inhibition of acetylcholinesterase by two genistein derivatives: kinetic analysis, molecular docking and molecular dynamics simulation. Acta Pharm Sin B. 2014 Dec;4(6):430-7. doi: 10.1016/j.apsb.2014.10.002.
22. Bartolini M, Bertucci C, Cavrini V, Andrisano V. beta-Amyloid aggregation induced by human acetylcholinesterase: inhibition studies. Biochem Pharmacol. 2003 Feb 1;65(3):407-16. doi: 10.1016/s0006-2952(02)01514-9.
23. Alam A, Shaikh S, Ahmad SS, Ansari MA, Shakil S, Rizvi SM, Shakil S, Imran M, Haneef M, Abuzenadah AM, Kamal MA. Molecular interaction of human brain acetylcholinesterase with a natural inhibitor huperzine-B: an enzoinformatics approach. CNS Neurol Disord Drug Targets. 2014 Apr;13(3):487-90. doi: 10.2174/18715273113126660163.
24. Islam MR, Zaman A, Jahan I, Chakravorty R, Chakraborty S. In silico QSAR analysis of quercetin reveals its potential as therapeutic drug for Alzheimer's disease. J Young Pharm. 2013 Dec;5(4):173-9. doi: 10.1016/j.jyp.2013.11.005.
25. Steiner T, Koellner G. Hydrogen bonds with pi-acceptors in proteins: frequencies and role in stabilizing local 3D structures. J Mol Biol. 2001 Jan 19;305(3):535-57. doi: 10.1006/jmbi.2000.4301.
26. Ahmad SS, Khalid M, Younis K. Interaction study of dietary fibers (pectin and cellulose) with meat proteins using bioinformatics analysis: An In-Silico study. LWT. 2020 Feb 1;119:108889.
27. Lineweaver H, Burk D. The determination of enzyme dissociation constants. Journal of the American chemical society. 1934 Mar;56(3):658-66.
28. Eadie GS. The inhibition of cholinesterase by physostigmine and prostigmine. Journal of Biological Chemistry. 1942 Nov 1;146(1):85-93.
29. Hanes CS. Studies on plant amylases: The effect of starch concentration upon the velocity of hydrolysis by the amylase of germinated barley. Biochem J. 1932;26(5):1406-21. doi: 10.1042/bj0261406.
30. DIXON M. The determination of enzyme inhibitor constants. Biochem J. 1953 Aug;55(1):170-1. doi: 10.1042/bj0550170.
31. Caldwell GW, Yan Z, Lang W, Masucci JA. The IC(50) concept revisited. Curr Top Med Chem. 2012;12(11):1282-90. doi: 10.2174/156802612800672844
32. Houghton PJ, Agbedahunsi JM, Adegbulugbe A. Choline esterase inhibitory properties of alkaloids from two Nigerian Crinum species. Phytochemistry. 2004 Nov;65(21):2893-6. doi: 10.1016/j.phytochem.2004.08.052.
33. Gutiérrez M, Arévaloa B, Martínezb G, Valdésa F, Vallejosc G, Carmonad U, Martine AS. Synthesis, molecular docking and design of Tetrahydroquinolines as acetylcholinesterase inhibitors. J Chem Pharm Res. 2015;7(3):351-8.
34. Pietsch M, Christian L, Inhester T, Petzold S, Gütschow M. Kinetics of inhibition of acetylcholinesterase in the presence of acetonitrile. FEBS J. 2009 Apr;276(8):2292-307. doi: 10.1111/j.1742-4658.2009.06957.x.
35. Nie F, Liang Y, Xun H, Sun J, He F, Ma X. Inhibitory effects of

tannic acid in the early stage of 3T3-L1 preadipocytes differentiation by down-regulating PPARγ expression. Food Funct. 2015 Mar;6(3):894-901. doi: 10.1039/c4fo00871e.

36. Jiang HZ, Quan XF, Tian WX, Hu JM, Wang PC, Huang SZ, Cheng ZQ, Liang WJ, Zhou J, Ma XF, Zhao YX. Fatty acid synthase inhibitors of phenolic constituents isolated from Garcinia mangostana. Bioorg Med Chem Lett. 2010 Oct 15;20(20):6045-7. doi: 10.1016/j.bmcl.2010.08.061.
37. Lim CC, Cook PJ, James IM. The effect of an acute infusion of vincamine and ethyl apovincaminate on cerebral blood flow in healthy volunteers. Br J Clin Pharmacol. 1980 Jan;9(1):100-1. doi: 10.1111/j.1365-2125.1980.tb04806.x.
38. Rassat J, Robenek H, Themann H. Changes in mouse hepatocytes caused by vincamin. A thin-sectioning and freeze-fracture study. Naunyn Schmiedebergs Arch Pharmacol. 1982 Mar;318(4):349-57. doi: 10.1007/BF00501177.
39. Pesce E, Viganò V, Piacenza G. Azione della vincamina sulla respirazione piastrinica [Effect of vincamine on platelet respiration]. Farmaco Prat. 1978 Aug;33(8):343-50.
40. Fayed AH. Brain trace element concentration of rats treated with the plant alkaloid, vincamine. Biol Trace Elem Res. 2010 Sep;136(3):314-9. doi: 10.1007/s12011-009-8550-3.
41. Daina A, Michielin O, Zoete V. SwissADME: a free web tool to evaluate pharmacokinetics, drug-likeness and medicinal chemistry friendliness of small molecules. Sci Rep. 2017 Mar 3;7:42717. doi: 10.1038/srep42717.
42. Lipinski CA, Lombardo F, Dominy BW, Feeney PJ. Experimental and computational approaches to estimate solubility and permeability in drug discovery and development settings. Adv Drug Deliv Rev. 2001 Mar 1;46(1-3):3-26. doi: 10.1016/s0169-409x(00)00129-0.
43. Veber DF, Johnson SR, Cheng HY, Smith BR, Ward KW, Kopple KD. Molecular properties that influence the oral bioavailability of drug candidates. J Med Chem. 2002 Jun 6;45(12):2615-23. doi: 10.1021/jm020017n.
44. Egan WJ, Merz KM Jr, Baldwin JJ. Prediction of drug absorption using multivariate statistics. J Med Chem. 2000 Oct 19;43(21):3867-77. doi: 10.1021/jm000292e.
45. Sánchez-Linares I, Pérez-Sánchez H, Cecilia JM, García JM. High-Throughput parallel blind Virtual Screening using BINDSURF. BMC Bioinformatics. 2012;13 Suppl 14(Suppl 14):S13. doi: 10.1186/1471-2105-13-S14-S13.